MICROSTRUCTURAL EVOLUTION OF AL 1100 ALUMINUM SUBJECTED TO SEVERE PLASTIC DEFORMATION

Gheorghe GURAU, Carmela GURAU
"Dunarea de Jos" University of Galati
email: ggurau@ugal.ro

ABSTRACT

The goal of this document is to promote a sequence of bulk-deformation processes able to produce ultrafine grain and also nanostructured wires with adequate length to be interesting for processing in metallurgical industry. Samples of aluminum Al 1100alloy (98.41 % Al) were subjected to repetitive Equal Channel Angular Pressing at room temperature in 1 to 4 passes. Severe deformed specimens were cold classical plastic deformed in wires. Microstructural evolution and mechanical properties were investigated. Optical microscopy progression is evaluated through a sequential interrupted process on each separate ECAP pass. The XRD studies reveal the influence of SPD on grain refinement of samples. A simply and new technology for obtaining intermediary products UFG and nanocristalline wires was developed.

KEYWORDS: SPD, ECAP, UFG, in bulk nanomaterials cold extrusion, aluminum alloys, microstructural evolution

1. Introduction

On October 18, 2011 the European Commission adopted the following definition of a nanomaterial: a natural material, made accidentally or manufactured, containing particles in the free, the aggregate or the agglomerate states and where 50% or more of the particles have size distribution, one or more dimensions, the size range 1 nm - 100 nm [1]. Under certain conditions described by the legislator, the percentage may drop below 50%.

In bulk nanostructures have all three dimensions at the nanometric scale (3-D). These categories of massive solids are nanometer-scale grains.

Severe plastic deformation are an important approach for manufactured metallic material in bulk, whose crystalline grain size varies from less then 100 nm or up to 200 nm for ultra-fine grained massive. The use of severe plastic deformation (SPD) for the processing of bulk ultrafine-grained and nanostructured materials is now extensive [2, 3, 4].

One of the successful top-down methods producing massive material with three dimensions at the nanoscale is ECAP (Equal Channel Angular Pressing). ECAP was first implemented in the 80s in the Soviet Union. ECAP uses a die where two channels are cut, equal in cross-section, intersecting at an inner angle denoted in literature with Φ, which is generally close to 90^0.

The sample is pressed around a sharp corner. ECAP introduces large plastic strains in metals and their alloys to reduce grain size, using repetitive pressing. The final ECAP products have nanometric grains or ultrafine grains, but keep the cross section and shape of the initial sample. ECAP is based on increasing the free energy of polycrystalline alloy initial coarse grain, through introduction of high density of defects, especially dislocations [5].

The properties of bulk nanostructured or UFG alloys differ very much from the polycrystalline ones with the same average chemical composition, massive with micrometer scale. Properties of nanomaterials depend on two very important factors: grain size and the number of atoms on the surface or in close proximity to the surface. In the case of ECAP, the grain size of the final product can be varied by controlling: die designed angles (Φ the inner angle and ψ the outer angle), pressure, number of successive passes, processing route. All factors described are impact in microstructure and homogeneity developments during process.

The properties of bulk nanomaterials depend on grain size distribution, boundary thickness and local chemical composition.

In the present work we studied an aluminum alloy, which especially displays the size and distribution influence of intermetallic compounds.

ECAP is a feasible process for bulk nanostructure or ultrafine grain materials. A major limit of method is represented by dimensions of deformed material. This paper has the major objective of promoting of technology capable to produce long wires with ultrafine structure and function on true deformation degree, nanometric bulk structure, in order to be implemented in industry. Therefore, the present work was targeted at employing two combined plastic deformation methods, ECAP plus direct extrusion, a desirable severe plastic deformation technology to perform in bulk nanostructured aluminum alloy wires.

2. Experimental procedure

This study was carried out on a commercial A 6061 aluminum alloy (composition of 0.87 % Si, 0.05%Mn, 0.05%Cu, 0.007%Zn, balance aluminum) supplied with rolled billets 10 mm x10 mm and cut at 10mmx10mm x50mm.

The billets were pressed in ECAP die with channel section 10mm x10 mm.

The specific die angles, inner Φ 90^0 and outer Y 13^0 determine effective strain 1.07 in one pass [6].

$$\varepsilon_{total} = \frac{1}{\sqrt{3}}\left[2\mathrm{ctg}\left(\frac{\Phi+\Psi}{2}\right)+\Psi\,\mathrm{cosec}\left(\frac{\Phi}{2}+\frac{\Psi}{2}\right)\right] \quad (1)$$

Replacing the values given in the above previous equation we will find:

$$\varepsilon_{total} = \frac{1}{\sqrt{3}}\left[2\mathrm{ctg}\left(\frac{90+13}{2}\right)+0.226\frac{1}{\sin\left(\frac{90}{2}+\frac{13}{2}\right)}\right]=1.07 \quad (2)$$

Specimens were pressed via route A at room temperature. Before pressing the samples were lubricated with a suspension of graphite in mineral oil to reduce friction. The constant pressing speed 17.3 mm/s was employed using a 20 tf press. After pressing, the die was rotated at 90^0 and the specimen was pressed back in the vertical channel.

Then another specimen pushes out the first one. Similarly, the ECAP process was conducted to obtain specimens with 1, 2, 3, and 4 passes, equivalent strain: 1.07, 2.14, 3.21, respectively 4.28. Following the ECAP procedure, eight samples were obtained, two with the same equivalent strain.

Four samples were used for investigations after severe plastic deformation and other four were deformed by direct cold extrusion. The direct extrusion die parameters are shown in Table 1.

The prismatic ECAP billets were pressed in the cylindrical die to obtain long UFG wires 4 mm in diameter.

Table 1

Diameter of container *D[mm]*	Diameter of calibrated zone *d [mm]*	Strain $\varepsilon = \frac{D^2 - d^2}{D^2}\times 100$	Equivalent strain $\varphi = \ln\frac{A_0}{A_1}$
15	4	92.88	2.64

The force variation in both processes, ECAP and direct extrusion, respectively, was monitored with Hottinger Spider 8 system and force-stroke data has been recorded. Micro-Vickers hardness measurements were made on ECAP and ECAP plus cold extrusion samples using a load of 0.9807 N and reported as mean of the three readings. The XRD characterization of the samples has been obtained with a RigakuDmax III-C system.

The optical microscopy study has been carried out using a microscope Olimpus BX45 with digital image resolution at higher magnifications. The scanning electron microscopy study has been carried out using a portable microscope SEM type Hitachi. Metallographic samples were processed in longitudinal section for ECAP deformed samples and cross sections for extruded samples and attacked to specific reagent: 0.5 ml HF, 1.5 ml HCl, 2.5 ml HNO3, 95.5 ml water.

3. Result and discussion

3.1. Pressures in ECAP and cold extrusion processes

In the ECAP process, the pressure increased continuously with stroke until the maximum is achieved, and then a decreasing variation take places. Toward the end of the ECAP process, pressure is almost constant. Figure 1 presents pressure versus stroke plot for effective plastic strain 4.28 respectively four ECAP passes. The maximum pressure, 446.94 MPa is also the maximum value reached in the ECAP process as shown in Table 2.

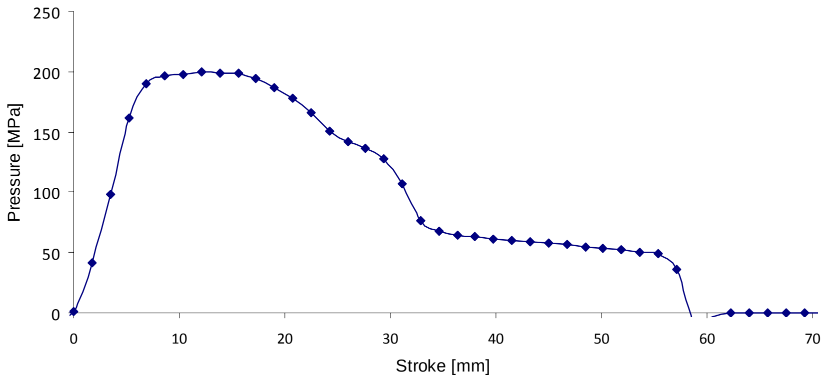

***Fig. 1.** Pressure versus stroke on fourth pass of ECAP – effective plastic strain 4.28*

Pressure in the cold direct extrusion process sowed different variation of pressure with stroke but specific for direct extrusion. At the start, a slow increase in pressure occurs suggesting cold pressing from prismatic shape to cylindrical shape, then the pressure increases rapidly to maximum.

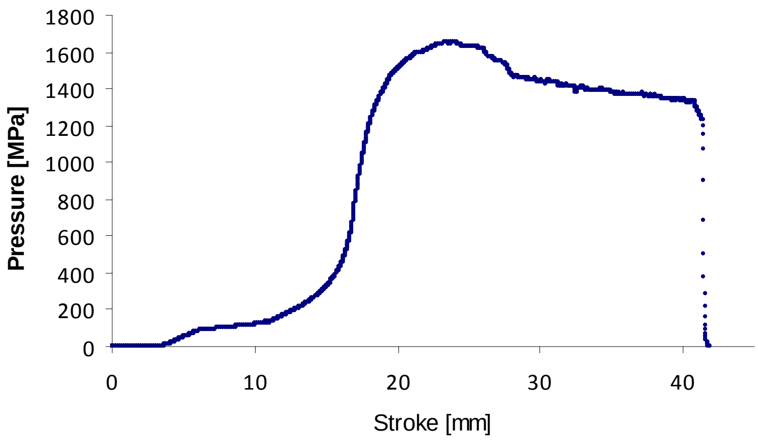

***Fig. 2.** Pressure versus stroke in cold direct extrusion process o ECAP billet after four passes-effective plastic strain 6.92*

In Figure 2, pressure versus stroke was plot for the cold extrusion process from four ECAP passes billet (effective plastic strain 6.92). The pressure increase up to 1.6 GPa almost four time higher than simply ECAP. When the maximum is reached, the pressure drops to lower values because the volume of the sample decreases in the container, the same as the friction forces.

Table 2 shows the maximum pressure values for different stages of ECAP and cold extrusion. It can be observed that the ECAP pressure increases from one pass to another and so does the conventional extrusion also. The values for ECAP + CE are higher than simply ECAP because of the accumulated strain and structure distortion.

Table 2

Processing route	**Maximum pressing pressure**
	[MPa]
Pass 1 ECAP	140.74
Pass 2 ECAP	231.75
Pass 3 ECAP	344.49
Pass 4 ECAP	446.94
Pass 1 ECAP + CE	1068.845
Pass 2 ECAP + CE	1220.434
Pass 3 ECAP + CE	1538.592
Pass 4 ECAP + CE	1650.242

3.2. Microhardness

At low temperatures, the increasing of grain boundaries behave as slip barriers, their area being far increased than in coarse grains bulk alloys. Therefore, nanocrystalline bulk metallic alloys are expected to have got value for mechanical resistance consistently higher than polycrystalline material with the same composition. Indeed at low temperatures, nanocrystalline materials were noted to become harder as the grains size is reduced [2, 5].

At elevated temperatures sliding grain boundaries and diffusion processes become meaningful. In the case of nanomaterials, a high density of imperfections and dislocations with different settlement at grain boundaries are specific. That affects significantly mechanical properties.

Due to their reduced grain size, and the increased number of atoms on surface, nanomaterials are expected to become more ductile at the same temperature then coarse grained polycrystalline alloys with the same composition.

In an up to date review on the mechanical behavior of UFG and nanocristalline materials [5] data is showed on normalized yield strength versus percentage elongation in tension for metals with grain sizes in the nanocrystalline range in comparison with UFG in cooper, titanium and aluminum alloys. Ultrafine grained materials (100–500 nm) exhibit increased yield strength along with good ductility in comparison to nanograined materials.

The plastic deformation of nanocrystalline materials is known to change as the grain size decreases into the ultrafine regime. This has been correlated to changes in strain hardening behavior at those grain sizes.

Ultrafine grain size can be described by a core-and-mantle model (grain-boundary limits with spacing of 10–100 nm). As the grain size is reduced, the ratio between volume fractions of the ''mantle'' and ''core'' increases, providing an increase in yield stress [5]. Microhardness values are presented in Figure 3. The values of severely plastically deformed ECAE samples with different degrees of deformation and measured values after extrusion in 4 mm wires were taken into account. Note that all samples ECAE plus extrusion the increase value of microhardness. The hardness value of the initial samples doubled from 337.6MPa to 678.8MPa. Severe plastic deformation leads to an advanced finishing structure.

As a consequence, hardness increases with the increase of deformation. Note the true deformation degree threshold value 3.21, above which plastic deformation by ECAP have no effect on mechanical properties. This correlates with the claims in literature that reveal that the mechanical behavior better marks ultrafine grain size than the nanometric structure.

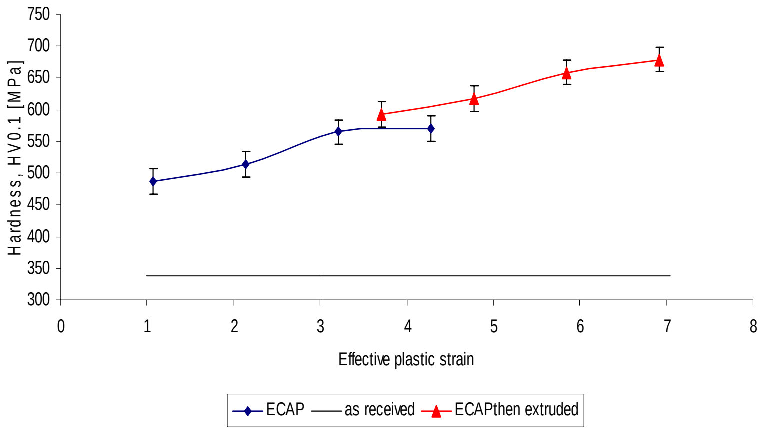

Fig. 3. *Variation of microhardness with the number of ECAP passes and ECAP+CE*

3.3. Microstructure evolution of Al 1100 alloy during the ECAP process

Samples of aluminum were investigated by optical microscopy, in as received state and after severe plastic deformation by the ECAP process with 1, 2, 3 and 4. The structure was analyzed after severe plastic deformation and ECAP plus subsequent direct extrusion 1 to 4 passes. Optical microscopy (OM) in as received sample of Al 1100 reveals a structure consisting of a coarse-grained solid solution and intermetallic compounds precipitated fine (Fig. 4). The solid solution presents polyhedral grain structure straight edges specific to fcc metals.

The microstructure highlighted slight unevenness grain size. Inside the crystalline grains of solid solution and on grain boundaries are observe several precipitates. Dark areas are insoluble phase Mg_2Si particles and Mg_2Al_3.

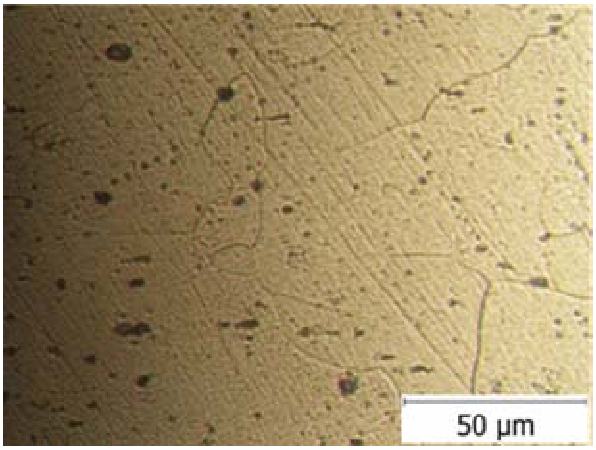

Fig. 4. *Microstructures of Al 1100 magnesium alloy in initial state*

Optical microscopy progression after severe deformation is evaluated through a sequential interrupted process on each separate ECAP pass. Evaluation was performed in 4 distinct regions of the samples severely deformed by ECAP for each 1 to 4 passes.

The four areas of microstructures billets outlining:

- input of the billet before deformation at entry in the die for next pass;
- plastic deformation zone, containing in the shear plane;
- deformed area after leaving the progressive shear zone;
- output end of the billet after current pass at leaving the die

The mode definition of these regions for samples severely deformed by the ECAP process are outlined in Figure 5.

The microstructural observation focused on characterization of the grain structure evolution with increasing number of passes, comparative in all the specific ECAP regions previous described.

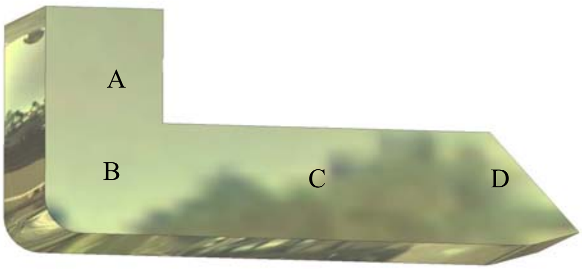

Fig. 5. *Regions of ECAP specimen observed by OM*

Optical images prevailed of the areas defined in Figure 5 for each of the four stages of processing by ECAP, using route A, are shown in Figures 5 - 8.

The deformation produced by ECAE is sequential, the shearing not being distributed in the entire billet simultaneously [7]. More than that, at every reinstatement of the sample in the die for a new deformation, the billet starts with a different texture, discontinuous in volume. But we can consider that deformation appears almost monotonically in a tight region around the shear plan defined by the die intersection plane [ec8]. This region, named plastic deformation zone, is not symmetric around the shear plan, and depends on all the ECAP process parameters.

3.3.1. Microstructure in region A

In the metallographic region A are shown the input of the billet before deformation, at entry in the die for next pass.

In the first ECAP pass, although in this region the material is not yet deformed, the microstructure displays a slightly deformed texture. The image in Fig. 6a is taken before the samples get in touch with the plastic deformation zone.

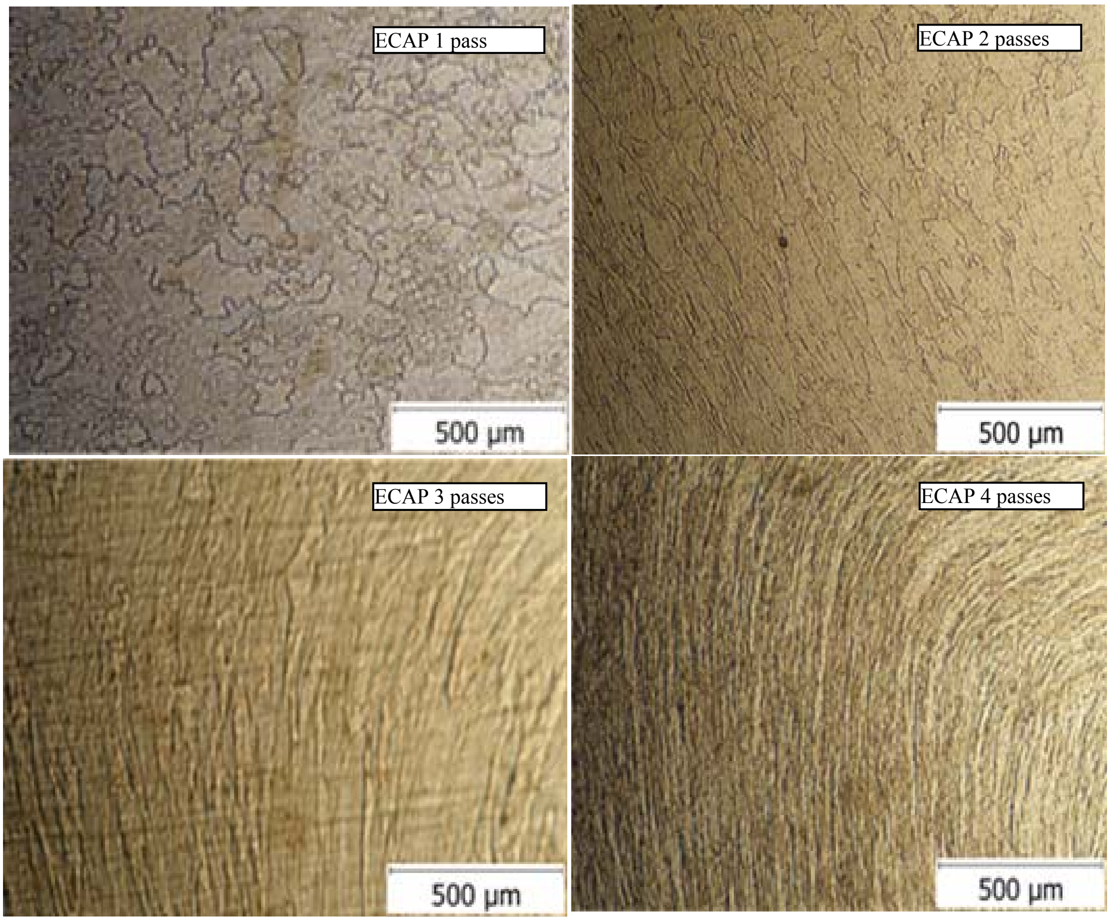

Fig. 6. *OM of ECAP billets after: one pass (a), 2 passes (b), 3 passes (c), 4 passes (d), Region A*

There is a solid solution rich in aluminum that shall grains easily elongated in the direction of application of force, in longitudinal section, on the outer surface of the sample which is in contact with the mold. The grains slightly flattened have dark particles of intermetallic compounds inside and at boundaries. The texture is only due to the contact of the sample with the mold walls. The billet was introduced initially lubricated all over the longitudinal contact with the mold. One possible reason is the effect of friction texture appearance can not be completely excluded. After two ECAP passes, the micrographic aspect reveals significant refinement of microstructure. Extended fine structure is formed then in the zone obtained after the first pass. Limits have parallel leaf appearance due to increased density of dislocations. After three ECAP passes grains, have an increasingly elongated and thin form. After four ECAP passes, just flow lines are observed. Crystalline grains are not OM observed, merely fibrous structure.

3.3.2. Microstructure in region B

Area noted with B is the plastic deformation zone that contain shear plane where plastic deformation occurs almost monotonously at the intersection of the two channels of the mold. At the first ECAP pass the crystalline grains of solid solution support a sinusoidal crimping process to shredding (Fig.7a).

In the following ECAP passes, the successive shearing of the grains already finished during the previous passages takes place. It forms a band structure aligned and finished growing, highlighting fiber flow lines. For all smaller grain sizes (d < 300 nm) shear band development is often observed to occur immediately after the onset of plastic deformation [9, 17].

The mechanism of grain-boundary rotation is one of several mechanisms that try to explain the modality of plastic deformation for ultrafine grains size metallic alloys [19, 11, 12]. The equiaxed grain structure is replaced by elongated grains through plastic deformation inside the shear band. Between two neighboring the barrier of boundary is eliminated by rotation so their orientation became closer together.

Similar mechanisms of grain boundary rotation and also based on dislocation generation at grain boundaries and in the limitrophe area for ultrafine grained size can explain how plastic deformation takes place.

TEM observation in Ti [13,14], Cu [15], Al–Li [16,18], and brass [19] in case of severe deformation grains, suggests applying mechanism of multiply dislocation that creating a work hardened layer close to the grain boundaries and in the same time grain boundary rotation.

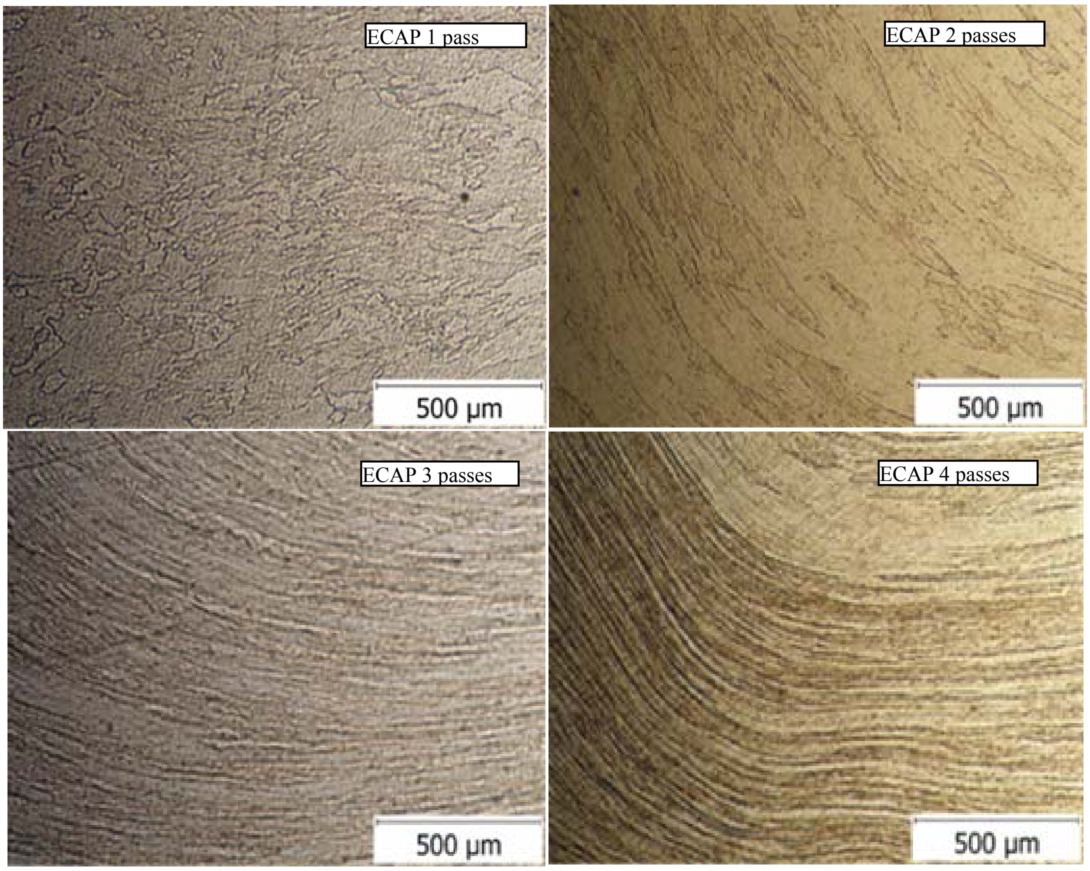

Fig. 7. *OM of ECAP billets Region B after one pass (a), 2 passes (b), 3 passes (c), 4 passes (d),*

3.3.3. Microstructure in region C

The output limit of the plastic zone area is defined in region C. The optical microstructure of the sample after each ECAP pass is presented in Figure 8. After one pass grains are elongated in the direction of deformation and strings as brittle intermetallic compound fine particles arranged along the slide can also be observed.

Increasing strain induces occurring significant microstructures differences.

Structure is becoming more elongated, finer and ultra finer grains size.

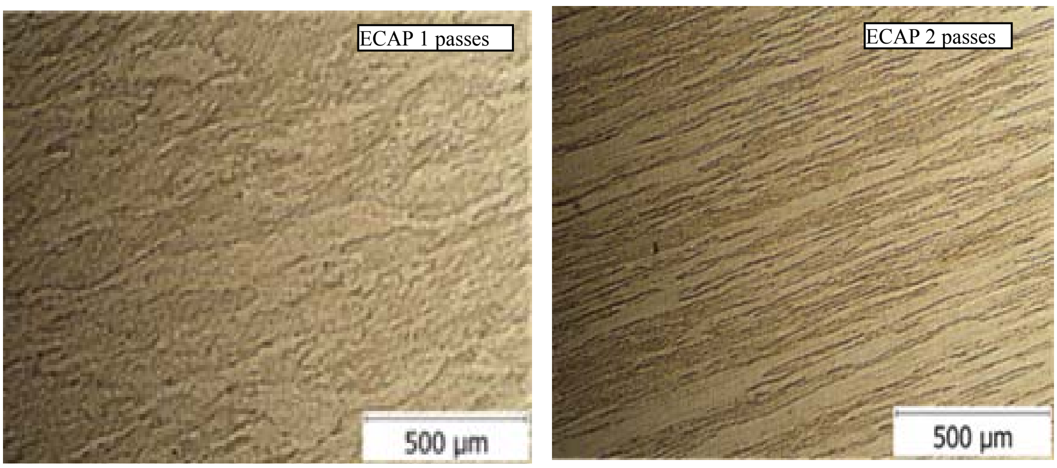

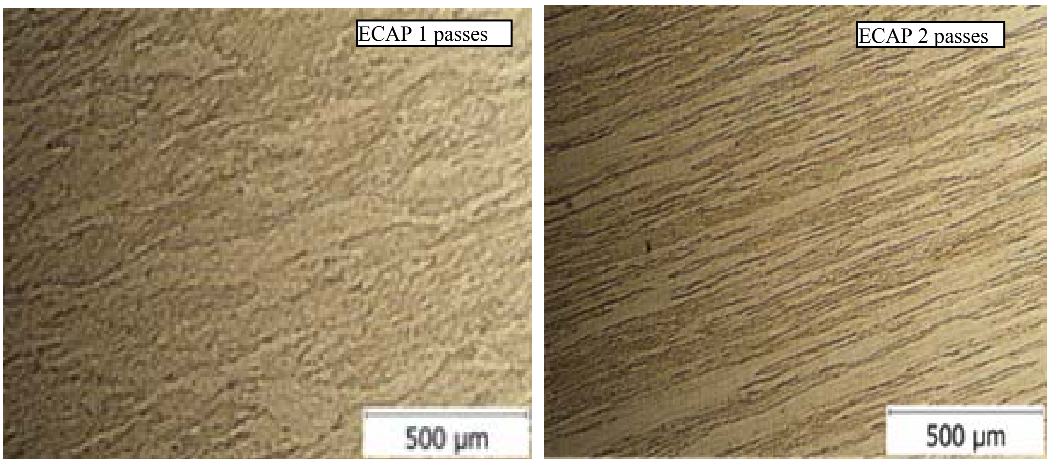

***Fig. 8.** OM of ECAP billets after: one pass (a), 2 passes (b), 3 passes (c), 4 passes (d), Region C*

The original grain boundaries disappear and are evident only fiber lines flow. As the deformation increases the fiber structure is compressed in transverse space, becoming more uniform and rotates to the direction of extrusion. The central area of the sample, defined by position in region C, have parallel fiber lines that lie at an angle of 65^0 from the vertical direction of extrusion.

The structure is consistent with the substructure quartz strip aligned with the shear plane direction.

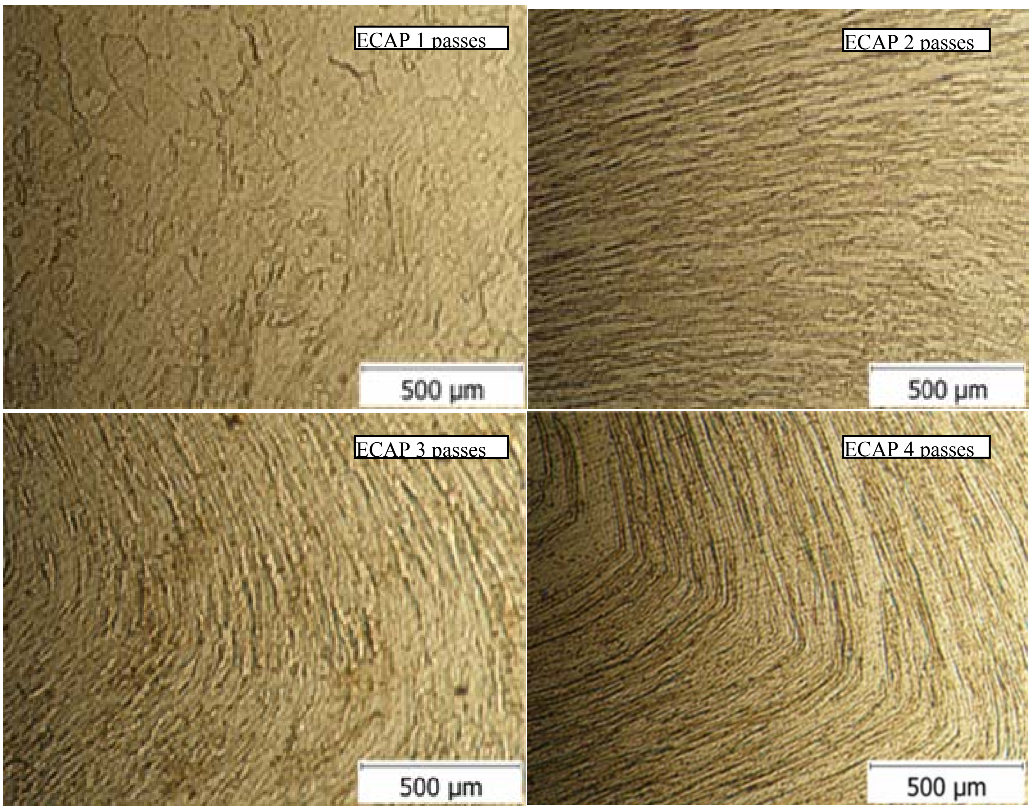

***Fig. 9.** OM of ECAP billets, Region D after: one pass (a), 2 passes (b), 3 passes (c), 4 passes (d)*

3.3.4. Microstructure in region D

With increasing plastic deformation in all areas observed by optical microscopy, regions A to D, the finishing of insoluble solid particles dark and gray colored (silicon, magnesium compounds and so on) occurs. Some authors believe that some of them dissolve in solid solution due to the thermal effect of ECAP severe plastic deformation.

In region D, the output end of the billet after current pass at leaving the die is revealed in Figure 8. After more than two ECAP passes, circular fibrous turns the deformation zone appear, a consequence of the uniformity deformation in the ECAP process.

3.3.5. SEM images in region C

SEM images reveal the same ultra dense material aspects after four ECAP passes. The microstructure has got fibrous appearance. Only flow lines and some coagulated precipitates can be seen (Fig 10).

The yield stress and tensile ductility are simultaneously adversely affected by porosity. The restriction, diminishing pores, in the ECAP deformed billet, provide a good behavior in terms of fracture, because of densification.

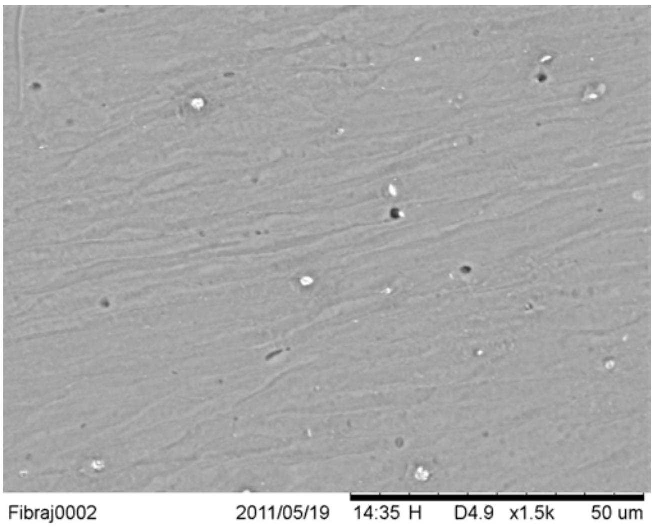

Fig. 10. *SEM micrograph ECAP four passes*

3.4. Microstructure evolution of Al 1100 alloy subjected to combined ECAP and direct extrusion

Samples severely plastically deformed by the ECAP method in one to four passes were subsequently plastic deformed by cold direct extrusion. Wires obtained after extrusion were studied by light microscopy in cross section. Figure 10 shows representative images obtained by OM after extrusion in one pass of the severely deformed semifinished ECAP samples, in one to four passes.

After extrusion of ECAP samples with 1.07 true deformation degrees, materials show the fine grain structure with corrugated and spiral shape (Fig 11 a).

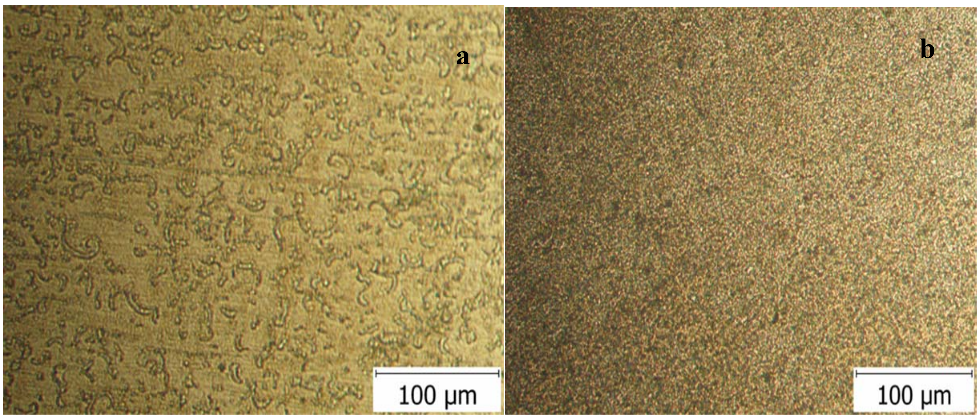

Fig. 11. *OM cold extruded wire one ECAP pass-a and 4 ECAP passes - b*

The increasing deformation degree by the ECAP process followed by classical extrusion in a single pass determine grain size finishing and also fibrous texture. Extruded samples after four ECAP deformations have only fiber lines (Fig.11b). The microstructure in Al1100 wires subjected to high strains ECAP plus Extrusion exhibited grain sizes in the 100–200 nm range.

4. Conclusions

A round-section wire start to square section samples severely deformed by ECAP can be produced, having ultrafine grain size after four ECAP passes and single cold extrusion.

A large increase in hardness for the nanocrystalline aluminum alloy samples made by the ECAP plus classical extrusion as compared to the annealed coarse-grained initial samples.

With the increment of true deformation degree from 1.07 to 4.28, the shape of the particle is changed firstly to become elongated and also corrugated, then it is reduced gradually until it simply becomes flow lines.

Pressing pass has a decisive influence on the microstructure evolution of aluminum alloy. With each increase of ECAP pass, the microstructure aspect is more dense and fibrous and finer. Subsequently, after leaving the plastic deformation zone, the grains are reoriented at 65^0 to the axis X in the shear direction. The ECAP microstructure evolution indicates a close relationship to simple shear deformation in region B and non-uniformity of deformation especially in region D. After extrusion of one ECAP pass samples, the structure presents the fine grain structure with corrugated and spiral shape. Extruded samples after four ECAP deformations have only fiber lines with dense surface aspect.

References

[1]. *** *Nanomaterials.* European Commission. Last updated 18 October (2011).

[2]. H. Gleiter - *Nanostructured Materials: Basicn Concepts, Microstructure and Properties,* Forschungszentrum Karlsruhe, Institut fur Nanotechnologie, Postfach 36 40, D-76021 Karlsruhe.

[3]. Ruslan Z. Valiev, Terence G. Langdon - *Principles of equal-channel angular pressing as a processing tool for grain refinement*, Progress in Materials Science 51 (2006) 881–981.

[4]. A. Azushima, R. Kopp, A. Korhonen, D.Y. Yang - *Severe plastic deformation (SPD) processes for metals*, Manufacturing Techology 37, (2008) 716-735.

[5]. M.A. Meyers et al. - Progress in Materials Science, 51 (2006) 427–556.

[6]. A.R. Eivani, A. Karimi Taheri - *A new method for estimating strain in equal channel angular extrusion*, Journal of Materials Processing Technology 183 (2007) 148-153.

[7]. A. A. Gadzer, F. Dalla Torre, C.F. Gu, C.H.J. Davies, E.V. Pereloma - *Microstructure and texture evolution of bcc metals subjected to equal channel angular extrusion*, Materials Science and Engineering 415 (2006), 126-139.

[8]. A. Gadzer, F. Dalla Torre, C. F. Gu, C. H. J. Davies, E. V. Pereloma - *Progressive structure during equal channel angular extrusion*, Materials Science and Engineering A 437 (2006) 259-267.

[9]. Wei Q, Kecskes L, Jiao T, Hartwig KT, Ramesh KT, Ma E. - Acta Mater (2004); 52:1859–69.

[10]. Jia D., Wang YM, Ramesh KT, Ma E, Zhu YT, Valiev RZ. - Appl Phys Lett (2001); 79:611–3.

[11]. Wang YM, Ma E., Chen M.W. - Appl Phys Lett (2002); 80:2395–7.

[12]. Jia D., Ramesh K.T., Ma E. - Scripta Mater (2000); 42:73.

[13]. Meyers M., Pak H.R. - Acta Mater (1986); 34:2493.

[14]. Meyers M.A., Subhash G., Kad B.K. -Prasad L. Mech Mater (1994); 17:175.

[15]. Andrade U.R., Meyers M.A., Vecchio KS, Chokshi AH. - Acta Metall Mater (1994);42:3183.

[16]. Chen R.W., Vecchio KS. -J Phys IV (1994); 4: C8-4591.

[17]. Murayama M, Howe JM, Hidaka H, Takaki S. - Science (2002); 295: 2433–5.

[18]. Xu Y.B., Zhong W.L., Chen Y.J., Shen L.T., Liu Q., Bai Y.L., et al. - Mater Sci Eng A, (2001); 299: 287.

[19]. Li Q., Xu Y.B., Lai Z.H., Shen L.T., Bai Y.L. - Mater Sci Eng A (2000); 276:127.